GOMOS ALGOM2s v1.0 Ozone Profiles using Two-step approach

Algorithm Theoretical Basis Algorithm

8 June 2016

Viktoria Sofieva (viktoria.sofieva@fmi.fi)

Finnish Meteorological Institute

CONTENTS

1 Introduction: document purpose

This ATBD describes the retrieval algorithm for ozone using night-time measurements by GOMOS/Envisat, which is optimized for the UTLS region. This algorithm for GOMOS ozone retrievals - ALGOM2s v 1.0 - has been developed within the framework of the ESA ALGOM project (GOMOS Level 2 evolution studies). It relies on the two-step retrieval approach as IPF v6 algorithm. This ATBD is distributed along with the corresponding dataset.

2 A short description of GOMOS measurements and the IPF v6.0 retrieval algorithm

Global Ozone Monitoring by Occultation of Stars (GOMOS) on board Envisat has performed about 440 000 night-time occultations during 2002–2012. Self-calibrating measurement principle, good vertical resolution and the wide vertical range from the troposphere up to the lower thermosphere make GOMOS profiles interesting for different analyses.

GOMOS is a stellar occultation instrument operating in UV-VIS-NIR wavelength region [*Kyrölä et al.*, 2004; *Bertaux et al.*, 2010]. The atmospheric transmission spectra, which are obtained after dividing the stellar spectra observed through the Earth atmosphere by the reference spectrum, recorded above the atmosphere, contain spectral features of absorption and scattering by gases and particles. Ozone, NO_2, NO_3, and aerosol extinction are retrieved from the UV-VIS spectrometer data. Ozone can be retrieved up to ~100 km, while other species are detectable in the stratosphere and in the upper troposphere. The lowest altitude of the GOMOS measurements depends on stellar brightness and the presence of clouds [*Tamminen et al.*, 2010]; it is usually between 5 and 20 km. The GOMOS IPF v.6 processing is described in detail in [*Kyrölä et al.*, 2010] and GOMOS ATBD (https://earth.esa.int/documents/10174/384988/GOMOS_ATBD_V3.pdf). Below we present the brief summary of the GOMOS IPF v6.0 retrieval algorithm.

2.1 GOMOS retrieval strategy

The GOMOS processing starts with various instrumental corrections, which are described in detail in [*Kyrölä et al.*, 2010]. First, the mean dark current is subtracted from the recorded spectra S_{obs}. Second, the reference star spectrum is averaged from sufficiently many measurements above the atmosphere, thus giving an accurate estimate of the star spectrum S_{star}. Then the spectrum observed through the atmosphere is divided by the reference spectrum, yielding the atmospheric transmission function:

$$T_{atm} = \frac{S_{obs}}{S_{star}} \qquad (1)$$

The component due to refractive effects is estimated and removed from the transmission data:

$$T_{ext} = \frac{T_{atm}}{T_{ref}} \quad (2)$$

The component T_{ref} includes estimates of both regular refractive effects (refractive attenuation, or dilution) and scintillations [*Dalaudier et al.*, 2001; *Sofieva et al.*, 2009]. The transmission spectra T_{ext} provide the basis for retrieval of atmospheric constituent densities. The transmission spectra can be modelled by using the well-known Lambert-Beer law

$$T_{\mathrm{ext}} = e^{-\tau} \quad (3)$$

where the optical depth τ is given by

$$\tau(\lambda) = \sum_j \int \sigma_j(\lambda, \mathrm{T}(\bar{r}(s)))\rho_j(\bar{r}(s))ds \quad (4)$$

Here the ρ_j's are constituent densities depending on the position $\bar{r}$ and the σ_j's are the temperature-dependent absorption or scattering cross sections (λ being wavelength). The integration is performed along the optical path joining the instrument and the source.

Ozone, NO_2, NO_3 and aerosol optical depth are retrieved from the UV-VIS spectrometer measurements. Since aerosol extinction spectrum is not known a priori, a second-degree polynomial model is used for the description of the aerosol extinction. The aerosol number density and two parameters that determine the wavelength dependence of aerosol extinction spectra are retrieved from GOMOS data. The study by Tamminen et al. (2010) has shown that the retrieval of GOMOS ozone profiles in the UTLS is highly sensitive to the aerosol model. In particular, using higher order (2^{nd} and 3^{rd} order) polynomial aerosol models results in ~30% larger ozone values in the UTLS and in the troposphere compared to the lower order model (zero or 1^{st} order). Due to non-orthogonality of cross-sections of Rayleigh scattering by air with the considered polynomial model of aerosol extinction, the air density is not retrieved from UV-VIS measurements by GOMOS. It is taken from ECMWF analysis data corresponding to occultation locations.

The GOMOS inversion from UV-VIS spectral measurements is split into two steps [*Kyrölä et al.*, 1993, 2010]. First, atmospheric transmission spectra are inverted into horizontal column densities *N* for gases and optical thickness for aerosols, for every ray perigee (tangent) altitude *h* (spectral inversion). Then, for every constituent, the collection of the horizontal column densities at successive tangent heights is inverted to vertical density profiles (vertical inversion). The use of the effective cross sections [*Sihvola*, 1994; *Kyrölä et al.*, 2010] allows the separation of the inversion problem into two parts. The two parts are, however, coupled together by the unknown effective cross sections. In order to take into account the coupling effect, the processing makes use of an iterative loop over spectral and vertical inversions.

2.2 Spectral inversion

The GOMOS spectral inversion problem can be written in the form:

$$\boldsymbol{T}_{ext} = \exp(-\boldsymbol{\Sigma N}) + \boldsymbol{\varepsilon} \quad (5)$$

where $\boldsymbol{T}_{ext}$ are measured transmittances after the correction of refractive effects at altitude *h*, ***N*** are horizontal column densities at this altitude, $\boldsymbol{\Sigma}$ is the matrix of effective cross-sections, and $\boldsymbol{\varepsilon}$ represents the error term (noise and modeling errors). The spectral inversion is performed for each tangent altitude separately (i.e., independently of other tangent altitudes). It relies on the standard maximum likelihood method, which is equivalent to minimization of the χ^2 statistics under the assumption of a Gaussian distribution of the measurement errors:

$$\chi^2 = \left(\boldsymbol{T}_{ext} - \boldsymbol{T}_{mod}(\boldsymbol{N})\right)^T \mathbf{C}^{-1} \left(\boldsymbol{T}_{ext} - \boldsymbol{T}_{mod}(\boldsymbol{N})\right) \qquad (6)$$

where $\boldsymbol{T}_{ext}$ is a vector of observed transmission spectra, $\boldsymbol{T}_{mod}$ is a vector of modeled transmittances, and **C** is the covariance matrix of transmission errors. The minimization of χ^2 is performed using the Levenberg-Marquardt algorithm [*Press et al.*, 1992], which provides both horizontal column densities ***N*** and a covariance matrix of their uncertainties $\mathbf{C}_N$. The covariance matrix of the transmission errors **C** is presented as a sum of two matrices:

$$\mathbf{C} = \mathbf{C}_{noise} + \mathbf{C}_{mod} \qquad (7)$$

where the diagonal matrix $\mathbf{C}_{noise}$ corresponds to the measurement noise and $\mathbf{C}_{mod}$ corresponds to the modeling error. The incomplete scintillation correction is the dominating source of modeling errors in the stratosphere. The scintillation correction errors are not correlated at different tangent altitudes, thus allowing the splitting of **C** into $\mathbf{C}_{noise}$ and $\mathbf{C}_{mod}$. They result in wavelength-dependent perturbations in the transmission spectra, therefore $\mathbf{C}_{mod}$ is essentially non-diagonal, its parameterization is presented in [*Sofieva et al.*, 2009]. The efficient numerical solution of the problem to minimize the χ^2 with the modelling error included is presented in [*Sofieva et al.*, 2010]. It has been shown that the normalized χ^2-values are close to unity [*Sofieva et al.*, 2010].

2.3 Vertical inversion

The vertical inversion aims to determine a vertical profile $x(z)$ that fulfils the equation

$$N(z) = \int \rho(z(s))ds \qquad (8)$$

where *N* is any of the horizontal column densities inverted in the spectral inversion and the integration is performed along the ray path. The problem is discretized by dividing the atmosphere into layers (the number of layers is set equal to the number of measurements in the occultation processed) and assuming the local densities to be linear functions of altitude between two successive GOMOS measurements. The vertical inversion in the matrix form can be written as

$$\mathbf{N} = \mathbf{K}\boldsymbol{\rho} + \boldsymbol{\varepsilon}_N \qquad (9)$$

where **K** is the forward model (kernel) matrix, **N** is a vector of measurements (horizontal column densities), **ρ** is a vector of unknowns (profile) and $\boldsymbol{\varepsilon}_N$ is a vector of horizontal column densities uncertainties. The vertical inversion is stabilized by Tikhonov-type regularization according to the

target resolution , which makes the vertical resolution practically independent of angles between the orbital plane and the direction to the star.

The target-resolution Tikhonov solution of $\mathbf{N} = \mathbf{K}\rho + \boldsymbol{\varepsilon}_N$ is given by

$$\hat{\rho} = (\mathbf{K}^T\mathbf{K} + \alpha\mathbf{H}^T\mathbf{H})^{-1}\mathbf{K}^T\mathbf{N} \qquad (10)$$

where the regularization matrix **H** is

$$\mathbf{H} = \mathrm{diag}\left[\frac{1}{h_i^2}\right]\begin{bmatrix} 0 & 0 & 0 & \ldots & 0 \\ 1 & -2 & 1 & \ldots & 0 \\ \ldots & \ldots & \ldots & \ldots & \ldots \\ \ldots & \ldots & 1 & -2 & 1 \\ 0 & 0 & 0 & \ldots & 0 \end{bmatrix}.$$

Here $\left[\frac{1}{h_i^2}\right]$ is shorthand to dividing all matrix elements by the square of the local altitude difference.

The regularization parameter α has been selected in such a way that the retrieved profiles have the desired target resolution. For ozone, the target resolution is 2 km below 30 km and 3 km above 40 km (with smooth transition between 30 and 40 km).

Since the vertical inversion is linear, the uncertainty of the retrieved profile is estimated through the standard error propagation.

3 ALGOM2s v1.0 retrieval algorithm

The main motivation for the development of an algorithm optimized on the UTLS region was the large positive ozone bias in the UTLS observed in validation of IPF v6 data (e.g., [*Hubert et al.*, 2015]). The main reason for such behavior is high sensitivity of the UTLS retrievals to an assumed aerosol extinction model.

The developed ozone retrieval algorithm – ALGOM2s v1.0 – provides ozone profiles in the whole GOMOS altitude range from the upper troposphere to the lower thermosphere. The inversion consists of the following steps:

1. Retrievals of horizontal column density ozone profile in the UTLS using visible triplets;
2. Forming the resulting horizontal column density ozone profile in the whole GOMOS range by combination of the V6 ozone profiles in the middle atmosphere and the new triplet ozone profile in the UTLS.
3. Performing the vertical inversion in the same way as in IPF V6.

Below we describe each step in detail.

3.1 Triplet inversion in the UTLS

We will use the wavelengths as in the classical triplet method by [*Flittner et al.*, 2000]: the reference wavelengths near 525 and 675 nm and absorbing wavelengths near 600 nm. Since stars are relatively

weak sources of light, several pixels are used for reference and absorbing wavelengths (Figure 1). Using differential optical depth allows nearly cancelling scintillation-dilution perturbations and a significant reduction of uncertainty due to Rayleigh scattering correction based on the ECMWF field. The Level 1 b transmission spectra $T_{L1b}(\lambda)$ at a given tangent altitude can be expressed as:

$$T_{L1b}(\lambda) = T_{ext}(\lambda) \cdot T_{dil}(\lambda) \cdot T_{sc}(\lambda), \tag{11}$$

where $T_{dil}(\lambda)$ and $T_{sc}(\lambda)$ are transmittances due to dilution and scintillation, respectively.

The differential optical depth $d\tau$:

$$\begin{aligned} d\tau &= \tau(\lambda_{ab}) - \tfrac{1}{2} \cdot \left(\langle \tau(\lambda_{r1}) \rangle + \langle \tau(\lambda_{r2}) \rangle \right) \\ \tau &= -\log(T_{L1b}) \end{aligned} \tag{12}$$

where λ_{ab} is absorbing wavelength, λ_{r1} and λ_{r2} are reference wavelengths, has contributions due to ozone absorption, Rayleigh and aerosol scattering, and due to refractive effects. However, due to the selected wavelengths, ozone contribution to the differential optical depth strongly dominates. This is illustrated in Figure 2, which compares the contributions of ozone absorption, Rayleigh scattering and dilution (refractive attenuation) to the differential horizontal optical depth for the visible triplet 525 nm, 602 nm, 675 nm. This means that Level 1b transmittances, without dilution and scintillation correction, can be used for the inversion from the visible triplets. The contribution from Rayleigh scattering to the differential optical depth is significantly smaller than that of ozone, but it can be as large as a few percent in the UTLS. Therefore, the Rayleigh optical depth is estimated (using the ECMWF field) and subtracted from the total optical depth data

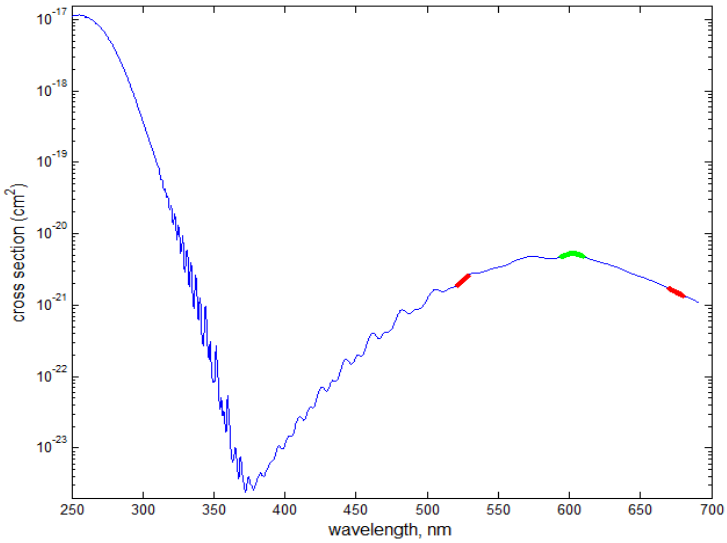

Figure 1. Reference (red, 521-529 nm and 670-680 nm) and absorbing (green, 592-612 nm) wavelengths.

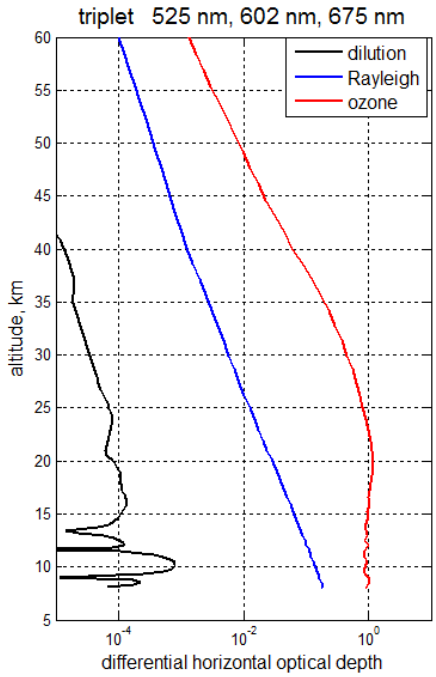

Figure 2. Differential horizontal optical depth for the visible triplet 525 nm, 602 nm, 675 nm due to ozone absorption, Rayleigh scattering and dilution. The contributions are computed based on the occultation R04078/S002.

Computation of optical depth (taking logarithm) requires good signal-to-noise ratio. Only the pixels with the signal-to-noise ratio larger than 3 are used in the inversion. The uncertainty of the optical depth σ_τ is approximated as:

$$\sigma_\tau = \frac{\sigma_T}{T}, \tag{13}$$

where σ_T is uncertainty of transmittance *T*.

The retrievals of ozone line density from Level 1b data using visible triplet are performed only in the UTLS, i.e., at altitudes below z_t+7 km, z_t is the tropopause height.

The average optical depth for reference channels $\langle \tau(\lambda_{r1}) \rangle$ and $\langle \tau(\lambda_{r2}) \rangle$ is used, and the triplet optical depth is computed for each channel at absorbing wavelengths 592-612 nm according to Eq.(12). The uncertainties of the differential optical depth values (Eq.(2)) are computed as:

$$\sigma_{d\tau}^2 = \sigma_\tau^2 + \frac{1}{4}\sigma_{r1}^2 + \frac{1}{4}\sigma_{r2}^2, \tag{14}$$

where σ_τ is uncertainty in the absorbing channel , σ_{r1} and σ_{r2} are uncertainties of the average optical depth in the reference channels.

Ozone line density is estimated for each pixel in absorbing channels $\mathrm{O}_3(\lambda) = d\tau(\lambda) / \mathrm{D}_{cross}(\lambda)$, where $\mathrm{D}_{cross}(\lambda)$ is the differential cross-sections corresponding to a triplet, and the weighted mean of these

estimates $\bar{\mathrm{O}}_3$ is computed (with weights inversely proportional to uncertainties $\sigma^2_{\mathrm{O3}}(\lambda_i)$ for individual absorbing channels). The associated uncertainty of the triplet line density $\bar{\mathrm{O}}_3$ is estimated as:

$$\sigma^2_{\bar{\mathrm{O}}_3} = \max\left(\frac{1}{\sum_{i=1}^{N} 1/\sigma^2_{\mathrm{O3}}(\lambda_i)} \cdot \frac{1}{(N-1)} \sum_{i=1}^{N} \frac{(\mathrm{O}_3(\lambda_i) - \bar{\mathrm{O}}_3)^2}{\sigma^2_{\mathrm{O3}}(\lambda_i)}, \frac{1}{\sum_{i=1}^{N} 1/\sigma^2_{\mathrm{O3}}(\lambda_i)} \right) \quad (15)$$

In Eq. (15), the factor $\frac{1}{\sum_{i=1}^{N} 1/\sigma^2_{\mathrm{O3}}(\lambda_i)}$ is the uncertainty of the weighted mean provided the uncertainties $\sigma^2_{\mathrm{O3}}(\lambda_i)$ are the only source of variations in ozone. The second factor in Eq. (15) takes into account variability between the different values of $\mathrm{O}_3(\lambda_i)$.

3.2 Combining V6 and triplet horizontal column densities

The combining V6 and triplet ozone profiles is performed in the UTLS (from 6 km above the tropopause down to the lowest altitude).

The uncertainty of V6 is modified by adding a function increasing linearly from 0% at (z_t+6 km) to 20% at the tropopause height z_t, with the saturation level of 20% below z_t (Figure 3, left, labelled as "V6 systematic"). Such modification characterizes the systematic uncertainty of V6 ozone line density due to uncertainty of the aerosol model. The combined ozone profile is the weighted mean of the V6 and triplet line density profiles with the weights inversely proportional to uncertainties: modified V6 uncertainty for V6 profile and $\sigma_{\bar{\mathrm{O}}_3}$ (Eq.(15)) for the triplet inversion (Figure 3, center). As a result, above (z_t + 6 km), ozone profile follows exactly V6 data. Below (z_t + 6 km), the profiles are closer to the triplet inversion and practically coincide with the triplet inversion at the tropopause and below (Figure 3, right).

If the lowest GOMOS altitude is above the tropopause, the triplet inversion is not performed and the profiles follow V6 data.

After combining the ozone line density profiles, the vertical inversion is performed in the same way as for V6. The detailed assessment and validation of the ALGOM2s v.1.0 data can be found in the dedicated Technical Note (Sofieva et al., 2016).

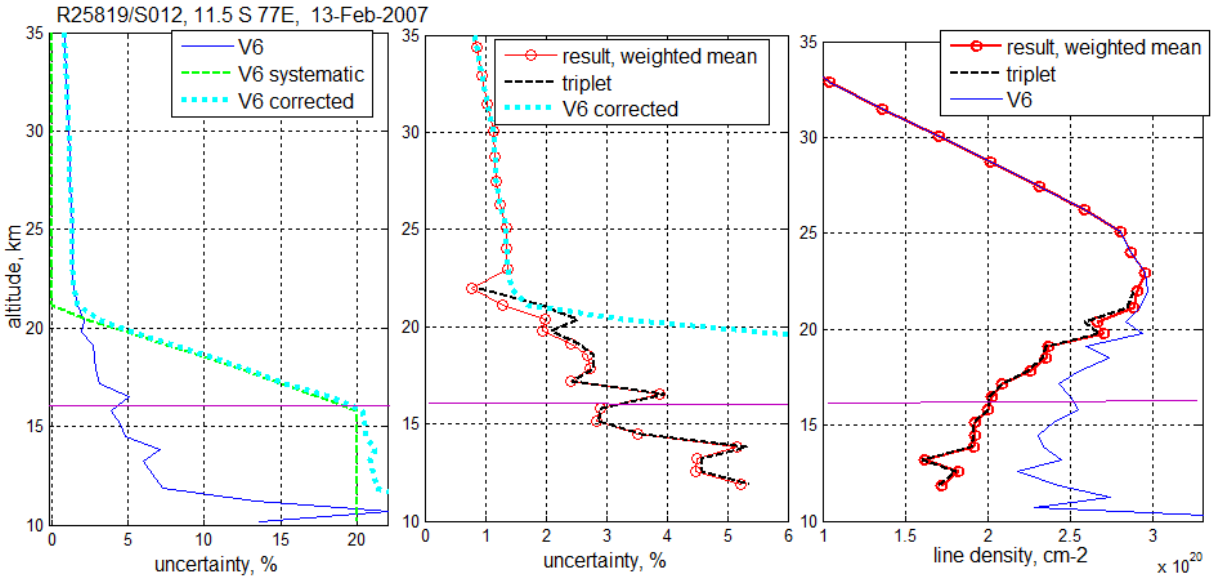

Figure 3. Illustration of combining triplet and V6 line density profiles using the data from occultation R25819/S012 (11.5°S 77°E, 13 February 2007). Left: Original uncertainty of V6 ozone line density (blue line), systematic uncertainty (green), which is added quadratically to the original V6 uncertainty, and the resulting corrected V6 uncertainty (cyan). Center: V6 corrected uncertainty (cyan, as in the left panel), the uncertainty of the triplet inversion (black) and the resulting uncertainty of the weighted mean of V6 and triplet profiles (red). Right: V6 ozone line density (blue), ozone line density from triplet inversion (black), and the weighted mean of V6 and triplet profiles (red). The lapse-rate tropopause height is ~16 km is indicated my magenta horizontal line.

3.3 GOMOS ozone profiles and their characterization

The GOMOS processors (both IPF v6 and ALGOM2s v1.0) provide ozone number density profiles on tangent-altitude grid. This grid depends of obliquity of occultation: the larger obliquity, the denser grid. However, the actual vertical resolution of GOMOS ozone profiles is the same in all occultations: 2 km below 30 km and 3 km above 40 km.

The stellar flux recorded by GOMOS, and thus signal-to-noise ratio and uncertainty of retrieved profiles, depends on stellar magnitude and spectral class. Since GOMOS IPF v6 and ALGOM2s v 1.0 ozone profiles coincide in the middle atmosphere, they have identical characterization there. The estimated random uncertainty of GOMOS ozone profiles is 0.5-5% in the stratosphere and 1-10% in the mesosphere and lower thermosphere. Validation of the uncertainty estimates for ozone profiles in the stratosphere has shown that they are realistic not dim stars [*Sofieva et al.*, 2014].

In the UTLS region, the uncertainty of the GOMOS ALGOM2s ozone profiles is a few tens of percent, depending on stellar brightness. For the brightest stars, the random uncertainty of GOMOS ozone profiles in the UTLS is ~10%.

4 References

Bertaux, J.-L. et al. (2010), Global ozone monitoring by occultation of stars: an overview of GOMOS measurements on ENVISAT, *Atmos. Chem. Phys.*, *10*(24), 12091–12148, doi:10.5194/acp-10-12091-2010.

Dalaudier, F., V. Kan, and A. S. Gurvich (2001), Chromatic refraction with global ozone monitoring by occultation of stars. I. Description and scintillation correction, *Appl. Opt.*, *40*(6), 866–877.

Flittner, D. E., P. K. Bhartia, and B. M. Herman (2000), O3 profiles retrieved from limb scatter measurements: Theory, *Geophys. Res. Lett.*, *27*(17), 2601–2604, doi:10.1029/1999GL011343. [online] Available from: http://dx.doi.org/10.1029/1999GL011343

Hubert, D. et al. (2015), Ground-based assessment of the bias and long-term stability of fourteen limb and occultation ozone profile data records, *Atmos. Meas. Tech. Discuss.*, *8*(7), 6661–6757, doi:10.5194/amtd-8-6661-2015. [online] Available from: http://www.atmos-meas-tech-discuss.net/8/6661/2015/

Kyrölä, E., E. Sihvola, Y. Kotivuori, M. Tikka, T. Tuomi, and H. Haario (1993), Inverse Theory for Occultation Measurements, 1: Spectral Inversion, *J. Geophys. Res.*, *98*, 7367–7381.

Kyrölä, E. et al. (2004), GOMOS on Envisat: An overview, *Adv. Sp. Res.*, *33*, 1020–1028.

Kyrölä, E. et al. (2010), Retrieval of atmospheric parameters from GOMOS data, *Atmos. Chem. Phys.*, *10*(23), 11881–11903, doi:10.5194/acp-10-11881-2010. [online] Available from: http://www.atmos-chem-phys.net/10/11881/2010/

Press, W. H., S. A. Teukolsky, W. T. Vetterling, and B. P. Flannery (1992), Numerical Recipes in FORTRAN, The Art of Scientific Computing, *Cambridge Univ. Press*, 933.

Sihvola, E. (1994), *Coupling of spectral and vertical inversion in the analysis of stellar occultation data*, Geophysical publications, no. 38, Finnish Meteorological Institute, Helsinki.

Sofieva, V. F., J. Tamminen, H. Haario, E. Kyrölä, and M. Lehtinen (2004), Ozone profile smoothness as a priori information in the inversion from limb measurements, *Ann. Geophys.*, *22*(10), 3411–3420.

Sofieva, V. F., V. Kan, F. Dalaudier, E. Kyrölä, J. Tamminen, J.-L. Bertaux, A. Hauchecorne, D. Fussen, and F. Vanhellemont (2009), Influence of scintillation on quality of ozone monitoring by GOMOS, *Atmos. Chem. Phys.*, *9*(23), 9197–9207.

Sofieva, V. F. et al. (2010), Retrievals from GOMOS stellar occultation measurements using characterization of modeling errors, *Atmos. Meas. Tech.*, *3*(4), 1019–1027, doi:10.5194/amt-3-1019-2010.

Sofieva, V. F. et al. (2014), Validation of GOMOS ozone precision estimates in the stratosphere,

Atmos. Meas. Tech., *7*(7), 2147–2158, doi:10.5194/amt-7-2147-2014. [online] Available from: http://www.atmos-meas-tech.net/7/2147/2014/

Tamminen, J., E. Kyrölä, and V. F. Sofieva (2004), Does prior information improve measurements?, in *Occultations for Probing Atmosphere and Climate - Science from the OPAC-1 Workshop*, edited by G. Kirchengast, U. Foelsche, and A. K. Steiner, pp. 87–98, Springer Verlag.

Tamminen, J. et al. (2010), GOMOS data characterisation and error estimation, *Atmos. Chem. Phys.*, *10*(19), 9505–9519, doi:10.5194/acp-10-9505-2010.